

Theory of Parametric Oscillator Threshold with Single-Mode Optical Masers and Observation of Amplification in LiNbO₃

G. D. BOYD AND A. ASHKIN

Bell Telephone Laboratories, Murray Hill, New Jersey

(Received 20 January 1966)

Theoretical and experimental results are given on cw parametric amplification and oscillation. Theoretical calculations incorporating Gaussian-mode theory into parametric-amplifier theory indicate that continuous parametric oscillation in LiNbO₃ using a gas-laser pump source should be achievable with tens of milliwatts of pump power. The requirements for achieving simultaneous resonance of signal and idler frequencies under phase-matched conditions for parametric oscillators are discussed. The effects of varying crystal temperature, electric field, and pump frequency to satisfy these requirements are included. The experiments involved the measurement of difference-frequency power at 0.9299 μ (10 754 cm⁻¹) produced in LiNbO₃ by mixing a signal at 1.1526 μ (8676 cm⁻¹) from the He-Ne laser with a pump at 0.5147 μ (19 430 cm⁻¹) from an argon ion laser. The LiNbO₃ crystal was adjusted in temperature so as to obtain phase matching normal to its optic axis, thus avoiding the deleterious effects of double refraction. The observed amplification was found to be in agreement with theory. Experimental results are given demonstrating low-loss resonators for the signal and idler frequencies, the loss being approximately 1% per pass. Data showing the dependence of optical path length in an optical resonator on temperature and electric field are given. The variation of the phase-matching condition with electric field is demonstrated in a second-harmonic-generation experiment.

1. INTRODUCTION

OPTICAL-parametric theory,¹ including the Gaussian transverse distribution² of single-mode laser beams is extended. From this theory with optimized parameters and the results of experiments on an optical-parametric amplifier and measurements of the Q of optical resonators, it is predicted that cw oscillation should be possible using gas-laser pump sources and LiNbO₃ as the nonlinear material.³ We estimate that a confocal resonator having a loss per pass of 1%, fabricated from single-domain^{4,5} LiNbO₃ should oscillate with a pump power of the order of 10 mW from the 0.5147- μ argon-ion laser in a single longitudinal and transverse mode. In previous work on parametric amplifiers⁶ and oscillators^{1,2,7-10} the power necessary to achieve observable gain or oscillation was large compared with power available continuously.

Parametric theory is cast in the same form as the theory of second-harmonic generation for Gaussian-mode beams as described previously^{11,12} and in papers

submitted^{13,14} for publication. The effects of double refraction,¹² diffraction,¹³ and mode coupling in resonators are included. The theory gives results for the gain per pass through the nonlinear medium for the case of a single-pass amplifier and also inside the resonant cavity of an oscillator. The difference between these gains makes it clear that pump sources that result in single-pass amplifiers with very small gain can still result in parametric oscillation.

The measurements on a single-pass amplifier and the Q of an optical resonator containing LiNbO₃ provide simple experimental checks on some of the elements of the theory used in making the threshold prediction and are thus useful preliminaries to the more complex cw-oscillator experiments.

Simultaneous resonance of the signal and idler frequencies is required if parametric oscillation is to be achieved. This requires some means of varying the optical path length of the resonator such as detached mirrors or, if one assumes that the signal-idler reflectors are attached to the crystal, temperature¹⁵ and electric field.^{9,10,16} Experimental results are given of the transverse electric field and temperature change required to produce a change in the optical path length of one-half wavelength along the resonator axis. The effect on simultaneous resonance of sweeping the pump frequency is also discussed.

The simultaneous resonance of the pump as well as that of the signal and idler is not discussed in this

¹ J. A. Armstrong, N. Bloembergen, J. Ducuing, and P. S. Pershan, *Phys. Rev.* **127**, 1918 (1962).

² R. H. Kingston and A. L. McWhorter, *Proc. IEEE* **53**, 4 (1965). These authors have also dealt with this problem using a different approach.

³ G. D. Boyd, R. C. Miller, K. Nassau, W. L. Bond, and A. Savage, *Appl. Phys. Letters* **5**, 234 (1964).

⁴ K. Nassau, H. J. Levinstein, and G. M. Loiacono, *Appl. Phys. Letters* **6**, 228 (1965).

⁵ K. Nassau and H. J. Levinstein, *Appl. Phys. Letters* **7**, 69 (1965).

⁶ C. C. Wang and G. W. Racette, *Appl. Phys. Letters* **6**, 169 (1965).

⁷ R. H. Kingston, *Proc. IRE* **50**, 472 (1962).

⁸ N. M. Kroll, *Phys. Rev.* **127**, 1207 (1962).

⁹ S. A. Akhmanov and R. V. Khokhlov, *Zh. Eksperim. i Teor. Fiz.* **43**, 351 (1963) [English transl.: *Soviet Phys.—JETP* **16**, 252 (1963)].

¹⁰ J. A. Giordmaine and R. C. Miller, *Phys. Rev. Letters* **14**, 973 (1965).

¹¹ A. Ashkin, G. D. Boyd, and J. M. Dziedzic, *Phys. Rev. Letters* **11**, 14 (1963).

¹² G. D. Boyd, A. Ashkin, J. M. Dziedzic, and D. A. Kleinman, *Phys. Rev.* **137**, A1305 (1965).

¹³ D. A. Kleinman, A. Ashkin, and G. D. Boyd, *Phys. Rev.* **145**, 338 (1966).

¹⁴ A. Ashkin, G. D. Boyd, and J. M. Dziedzic, *IEEE J. Quantum Electron.* (to be published).

¹⁵ R. C. Miller, G. D. Boyd, and A. Savage, *Appl. Phys. Letters* **6**, 77 (1965).

¹⁶ G. E. Peterson, A. A. Ballman, P. V. Lenzo, and P. M. Bridenbaugh, *Appl. Phys. Letters* **5**, 62 (1964).

paper. One problem encountered when considering resonance of the pump¹⁴ is that of matching the laser pump source into the external resonator, unless the nonlinear crystal is placed within the laser, which involves other difficulties. Another, which is also met in second-harmonic double resonance,² is to obtain the proper spatial relation between the resonance of the polarization wave and the electromagnetic wave it radiates. At worst this can result in no amplification because of the opposite effect of waves traveling in both directions.

2. THEORY

2.1. Single-Pass Parametric Amplifier

Consider a parametric amplifier in which a pump wave of power P_3 and a signal wave of power P_1 are incident on a LiNbO₃ crystal of length l in the X crystal direction (\mathbf{a} axis). Operation normal to the optic axis is selected here since the effects of double refraction¹² are absent in this case. The calculation is made in the near field where diffraction is negligible. Diffraction will be included approximately later in the discussion of parametric threshold. The calculation follows the theory of BADK.¹² In this method the transverse variation of the field is taken into account by summing the radiation from each incremental volume of polarization over the Gaussian-beam cross section.

When the signal and idler beams travel approximately in the X crystal direction normal to the crystal optic axis Z , the nonlinear polarizations at frequencies ω_1 and ω_2 are related to the components of electric field along the X, Y, Z crystal axis at frequencies $\omega_1, \omega_2, \omega_3$ by

$$\mathcal{O}_{1Y^0} = 2d_{15}E_{2Y^0}E_{3Z^0}, \quad \mathcal{O}_{2Y^0} = 2d_{15}E_{1Y^0}E_{3Z^0}, \quad (2.1)$$

where d_{15} is the appropriate term of the nonlinear tensor previously defined³ and $\omega_3 = \omega_1 + \omega_2$. The superscripts o and e stand for ordinary and extraordinary and indicate the direction of the electric field and polarization vectors relative to the crystal axis. In (2.1) \mathcal{O} and E represent Fourier amplitudes following Kleinman's definition.^{17,18} Thus, the nonlinear polarization in (2.1) is *not* an instantaneous polarization. This can be a confusing point since some authors define the nonlinear coefficient in terms of the instantaneous (time-dependent) polarization as will be mentioned later.

We shall assume throughout this paper that all three frequency beams are collinear and phase matched, i.e., $k_3 = k_1 + k_2$. Furthermore define an x, y, z beam coordinate system with the z axis the direction of propagation (i.e., $z = X$) with $y = Y$ and $x = -Z$. In the experimental section we shall allow z to make an angle $\theta \lesssim 90^\circ$ with the Z crystal axis so as to adjust for phase match at $\theta = \theta_m$. It is assumed that $\theta_m = 90^\circ$ in all the

theoretical treatment; experimentally it is always very close to 90° .

The radial variation in the transverse electric field of a Gaussian beam in the near field of the TEM₀₀ mode is represented by¹⁹

$$E_i(r, z) = E_{i0}(z)e^{-r^2/w_i^2}, \quad i=1, 2, 3, \quad (2.2)$$

where w_i is the beam radius at frequency ω_i . In treating a three-dimensional problem the polarizations and electric fields of (2.1) are allowed to be functions of r and z where $r^2 = x^2 + y^2$. The signal, idler and pump frequencies may be defined in terms of the degenerate frequency ω_0 as

$$\omega_1 = \omega_0(1 - \gamma), \quad \omega_2 = \omega_0(1 + \gamma), \quad \omega_3 = 2\omega_0. \quad (2.3)$$

When the pump has the proper phase relative to the signal and idler (i.e., when the signal and idler are simultaneously maximum the pump leads by 90°) then it is straightforward to show from Maxwell's equations with a polarization source term that the spatial rates of change of the amplitudes of the electric fields in unrationalized esu are

$$k_1[\partial E_1(r, z)/\partial z] = 2\pi(\omega_1^2/c^2)\mathcal{O}_{1Y^0}(r), \quad (2.4)$$

$$k_2[\partial E_2(r, z)/\partial z] = 2\pi(\omega_2^2/c^2)\mathcal{O}_{2Y^0}(r). \quad (2.5)$$

The above may be conveniently written in terms of a gain parameter $g(r)$ as follows

$$\partial E_1(r, z)/\partial z = g(r)(\omega_1 n_2/\omega_2 n_1)^{1/2}E_2(r, z), \quad (2.6)$$

$$\partial E_2(r, z)/\partial z = g(r)(\omega_2 n_1/\omega_1 n_2)^{1/2}E_1(r, z), \quad (2.7)$$

where

$$g(r) = (\omega_1 \omega_2 / n_1 n_2)^{1/2} (2\pi/c) (2d_{15}) E_3(r). \quad (2.8)$$

From (2.1) one can see that the effect of mixing two Gaussian beams of radii w_1 and w_3 is to produce a polarization distribution of radius w_2 where

$$1/w_2^2 = 1/w_1^2 + 1/w_3^2 \quad (2.9)$$

and likewise if we mix beams of radii w_2 and w_3 we produce a polarization distribution of radius w_1 , where

$$1/w_1^2 = 1/w_2^2 + 1/w_3^2. \quad (2.10)$$

The solutions of (2.6) and (2.7) satisfying the boundary conditions of no idler electric field at $z=0$ in the region $0 \leq z \leq l$ and in the small-gain approximation are

$$\bar{E}_1(r, z) = E_1(r, 0) \cosh gz \approx E_1(r, 0) [1 + \frac{1}{2}(gz)^2], \quad (2.11)$$

$$\bar{E}_2(r, z) = \left(\frac{n_1 \omega_2}{n_2 \omega_1} \right)^{1/2} E_1(r, 0) \sinh gz \approx \left(\frac{n_1 (1 + \gamma)}{n_2 (1 - \gamma)} \right)^{1/2} \times E_1(r, 0) [gz], \quad (2.12)$$

where the idler field $\bar{E}_2(r, z)$ is in the mode characterized by the beam radius w_2 . $\bar{E}_1(r, z)$ is the sum of two modes of radius w_1 and w_1 .

¹⁷ D. A. Kleinman, Phys. Rev. **126**, 1977 (1962).

¹⁸ D. A. Kleinman, Phys. Rev. **128**, 1761 (1962).

¹⁹ G. D. Boyd and J. P. Gordon, Bell System Tech. J. **40**, 489 (1961); G. D. Boyd and H. Kogelnik, *ibid.* **41**, 1347 (1962).

To find the power as a function of z in this parametric amplification process one must substitute the radial variations of Gaussian beams and integrate over the transverse coordinates. In (2.8) the gain per unit length is proportional to the pump electric field and is given by

$$g = g_0 e^{-r^2/w_3^2}, \quad (2.13)$$

where

$$g_0^2 = K(1-\gamma^2)(P_3/2w_3^2), \quad (2.14)$$

$$K = \frac{128\pi^2\omega_0^2(2d_{15})^2}{n_1n_2n_3c^3} \quad (2.15)$$

and the pump power in unrationalized esu is given by

$$P_3 = (n_3c/16)E_{30}^2w_3^2, \quad (2.16)$$

which is independent of z since we neglect pump depletion.

After integrating over the beam radius the resultant signal and idler powers at $z=l$ are given by

$$P_1(l) - P_1(0) = K \frac{P_3 P_1(0)}{2} (1-\gamma^2) \frac{l^2}{w_1^2 + w_3^2}, \quad (2.17)$$

$$\bar{P}_2(l) = K \frac{P_3 P_1(0)}{2} (1+\gamma)^2 \frac{l^2}{w_1^2 + w_3^2}. \quad (2.18)$$

Equation (2.18) will be compared with experiment in Sec. 3.1.

2.2. Parametric Oscillator Threshold

Consider a parametric oscillator in which signal and idler are simultaneously resonant and the pump is assumed to make a single pass with no depletion. After many traversals of the resonator the $e^{+\sigma z}$ solution for signal and idler dominates over $\cosh gz$ and $\sinh gz$. We shall calculate the gain per pass assuming steady-state oscillation and then equate this gain to the loss so as to obtain the pump power threshold for parametric oscillation. Assume that the signal and idler resonator eigenfunctions have radii w_1 and w_2 which cannot, for finite w_3 , be equal to \bar{w}_1 and \bar{w}_2 as defined by (2.10) and (2.9). An expansion of the \bar{w}_2 mode in terms of w_2 eigenfunctions of the type (2.2) leads to a coupling coefficient²⁰ between the lowest order modes which relates the electric fields on the axis by

$$w_2 E_{20} = c_{00}^2 \bar{w}_2 \bar{E}_{20}, \quad (2.19)$$

where

$$c_{00}^2 = \frac{2w_2}{\bar{w}_2 \{1 + (w_2/\bar{w}_2)^2\}}. \quad (2.20)$$

A similar definition applies for the coupling coefficient to the w_1 mode.

In a steady-state condition of parametric oscillation the signal and idler electric fields are in modes with

²⁰ H. Kogelnik, in *Proceedings of the Symposium on Quasi-Optics* (Polytechnic Press, Brooklyn, 1964), Vol. 14, pp. 333-347.

beam radii w_1 and w_2 and are characterized by the magnitude of the transverse-electric-field strengths E_{10} and E_{20} at $r=0$. These will mix with the pump electric field E_{30} in a mode of radius w_3 to give *increments* in the signal and idler electric fields in modes with beam radii \bar{w}_1 and \bar{w}_2 . From (2.6), (2.7), etc. the spatial rate of growth of the signal and idler frequencies are given by

$$\begin{aligned} \partial \bar{E}_1(r)/\partial z &= g_0 (\omega_1 n_2 / \omega_2 n_1)^{1/2} E_{20} e^{-r^2/\bar{w}_1^2}, \\ \partial \bar{E}_2(r)/\partial z &= g_0 (\omega_2 n_1 / \omega_1 n_2)^{1/2} E_{10} e^{-r^2/\bar{w}_2^2}, \end{aligned} \quad (2.21)$$

where \bar{w}_1 and \bar{w}_2 are given by (2.10) and (2.9). Since we are considering only the situation of small gain, E_{10} and E_{20} within the signal and idler resonator are approximately independent of z .

Only the fraction of the increment idler electric field $\partial \bar{E}_2(r)/\partial z$ coupled into the TEM₀₀ mode with radius w_2 is useful. This coupling factor is most usefully thought of as the coefficient resulting from an expansion of the polarization distribution of (2.4) and (2.5) in terms of the complete set of modes characterized by w_1 and w_2 . Only the polarization in the TEM₀₀ mode is useful since the higher order modes have different phase velocities and thus will not be simultaneously resonant with the TEM₀₀ mode except in the very special circumstance of an exact confocal resonator. Applying the coupling coefficient from (2.19) to (2.21) gives the incremental increase in the signal and idler electric fields in the TEM₀₀ resonator mode.

$$\begin{aligned} \partial E_1(r)/\partial z &= g_0 c_{00}^2 (\bar{w}_1/w_1) (\omega_1 n_2 / \omega_2 n_1)^{1/2} E_{20} e^{-r^2/w_1^2}, \\ \partial E_2(r)/\partial z &= g_0 c_{00}^2 (\bar{w}_2/w_2) (\omega_2 n_1 / \omega_1 n_2)^{1/2} E_{10} e^{-r^2/w_2^2}. \end{aligned} \quad (2.22)$$

c_{00}^2 in (2.22) are for frequencies ω_1 and ω_2 , respectively.

The incremental power gain in the idler mode can be computed in the approximation of small gain as

$$\frac{\partial P_2}{\partial z} = \frac{n_2 c}{8\pi} \int_0^\infty 2E_2(r) \frac{\partial E_2(r)}{\partial z} 2\pi r dr, \quad (2.23)$$

where it is assumed that the bulk crystal loss is small enough to be combined with the mirror losses. From (2.2), (2.22), and (2.23) one obtains for the idler, and likewise the signal mode, the relations

$$\begin{aligned} \partial P_2/\partial z &= (KP_1 P_2 P_3)^{1/2} (1+\gamma) M, \\ \partial P_1/\partial z &= (KP_1 P_2 P_3)^{1/2} (1-\gamma) M, \end{aligned} \quad (2.24)$$

where

$$M = \sqrt{2} \frac{\bar{w}_2 c_{00}^2}{w_1 w_3} = \frac{2\sqrt{2} w_1 w_2 w_3}{w_1^2 w_2^2 + w_1^2 w_3^2 + w_2^2 w_3^2}. \quad (2.25)$$

M is seen to be symmetrical in w_1 and w_2 . Maximization of $M(w_3)$ yields

$$M_m = [2/(w_1^2 + w_2^2)]^{1/2} \quad (2.26)$$

at

$$1/w_3^2 = 1/w_1^2 + 1/w_2^2, \quad (2.27)$$

It should be mentioned that (2.24) can be obtained directly without use of coupling coefficients if in (2.23) we integrate over the $\partial \bar{E}_2(r)/\partial z$ electric field in the w_2 mode instead of integrating over $\partial E_2(r)/\partial z$. This accomplishes the expansion directly.

The relation (2.27) between the optimum beam radius of the pump and the radii of the signal and idler modes has an important implication in the more general case when diffraction is not neglected. Let n_1, n_2, n_3 be the refractive indices at the frequencies involved and n_0 the average of n_1 and n_2 corresponding approximately to the degenerate frequency. Then

$$n_1 = n_0(1 - \zeta), \quad n_2 = n_0(1 + \zeta). \quad (2.28)$$

Phase matching requires that

$$n_3 = n_0(1 + \gamma\zeta). \quad (2.29)$$

In terms of the confocal parameter b_1, b_2 of the signal and idler modes, respectively, one finds

$$\frac{1}{w_1^2} + \frac{1}{w_2^2} = \frac{b_0}{w_0^2} \left\{ \frac{(1 - \gamma)(1 - \zeta)}{b_1} + \frac{(1 + \gamma)(1 + \zeta)}{b_2} \right\}, \quad (2.30)$$

where

$$\begin{aligned} w_0^2 &= b_0 c / n_0 \omega_0, & w_3^2 &= b_3 c / n_3 2\omega_0 \\ w_1^2 &= b_1 c / n_1 \omega_1, & w_2^2 &= b_2 c / n_2 \omega_2. \end{aligned} \quad (2.31)$$

In the most practical resonator for a parametric oscillator, signal and idler share the same reflector surfaces and thus have the same surfaces of constant phase and confocal parameter. Thus let

$$b_0 = b_1 = b_2. \quad (2.32)$$

From (2.27), (2.29), (2.30), and (2.31) one obtains

$$b_3 = b_0. \quad (2.33)$$

This implies that the surfaces of constant phase of the pump signal and idler, optimized for the near field according to (2.27), coincide in the far field as well as the near field. Furthermore with the confocal-beam parameters all the same, the three beams spread at the same rate and the ratio of their beam radii remains constant from the near to far field. Thus if we consider the inclusion of diffraction effects in the parametric-oscillator-threshold calculation it is apparent that the pump-size optimization given by (2.27) as obtained for the near field is also valid in the far field.

Using (2.24) and (2.26) we compare the gain per pass through a crystal of length l for the parametric oscillator $\Delta P_2 / (P_1 P_2)^{1/2} = (K P_3)^{1/2} (1 + \gamma) \sqrt{2} / (w_1^2 + w_2^2)^{1/2}$ (2.34) with the single-pass-parameter amplifier gain from (2.18)

$$\bar{P}_2 / P_1 = K P_3 (1 + \gamma)^2 l^2 / 2(w_1^2 + w_2^2). \quad (2.35)$$

In (2.34) $P_1 \approx P_2$ in the oscillator and thus, neglecting small factors, the gain for the amplifier is roughly the square of that of the oscillator and therefore much

smaller for small gains. Consequently oscillator thresholds are achieved at pump power levels that would yield only insignificant parametric-amplifier gains.

From (2.24) note that the increments in the signal and idler power $\Delta P_1, \Delta P_2$ satisfy the well-known Manley-Rowe condition of

$$\Delta P_2 / \Delta P_1 = (1 + \gamma) / (1 - \gamma) = \omega_2 / \omega_1. \quad (2.36)$$

The parametric-oscillator-threshold condition is dependent upon the resonator losses. Let ϵ_1 and ϵ_2 be the equivalent one-way loss of the signal and idler modes

$$\delta P_1 / P_1 = -\epsilon_1, \quad \delta P_2 / P_2 = -\epsilon_2. \quad (2.37)$$

Therefore in the steady-state condition of parametric oscillation the ratio of power in the idler and signal modes is

$$\frac{P_2}{P_1} = \frac{1 + \gamma \epsilon_1}{1 - \gamma \epsilon_2}. \quad (2.38)$$

To obtain the pump power threshold condition, within the framework of our near-field assumption, we equate the round-trip loss of the signal and idler to the one-way power gain assuming that the pump traverses the resonator only in one direction.

$$P_3 = \frac{4\epsilon_1\epsilon_2}{K(1 - \gamma^2)[2l^2 / (w_1^2 + w_2^2)]} \quad (2.39)$$

using the optimum pump-beam radius given by (2.27). For the degenerate ($\gamma = 0$) equal-loss ($\epsilon_1 = \epsilon_2$) situation this is in agreement with Kingston and McWhorter.² Note that they define the nonlinear coefficient in terms of the product of time-dependent fields and consequently $2d_{15} = \chi^{231} / 2$. (They use $\omega_1 = \omega_2 + \omega_3$.)

Under the conditions of (2.32) where signal and idler share the same surfaces of constant phase one can obtain

$$\frac{2l^2}{w_1^2 + w_2^2} = \frac{l^2}{w_0^2} \frac{(1 - \gamma^2)(1 - \zeta^2)}{1 + \zeta\gamma}. \quad (2.40)$$

Consequently (2.39) can be written

$$P_3 = \frac{4\epsilon_1\epsilon_2(1 + \zeta\gamma)}{K(1 - \gamma^2)^2(1 - \zeta^2)(l^2/w_0^2)}. \quad (2.41)$$

Clearly the threshold power P_3 is reduced as one increases the ratio l^2/w_0^2 until diffraction can no longer be neglected. Study of second-harmonic generation (SHG) from focused beams¹³ shows that effective interaction occurs over roughly the confocal distance b of the fundamental beam. For purposes of making an estimate let $l/b_0 = 1$. Consequently

$$l^2/w_0^2 = l k_0 (l/b_0) \rightarrow l k_0. \quad (2.42)$$

For $l = 1$ cm this yields a value of $l/w_0 = 368$. The parametric-oscillator threshold is thus inversely pro-

portional to crystal length assuming reflector losses dominate over bulk-crystal losses.

To estimate the parametric-oscillator pump threshold we must evaluate K from (2.15). For single-domain LiNbO_3 it was found⁸ that $d_{15}(\text{LiNbO}_3) \approx 11d_{14}(\text{KDP})$ and for KDP the nonlinear coefficient¹¹ $d_{14} \approx 2 \times 10^{-9}$ esu where we have allowed for the longitudinal modes present in that experiment by reducing d_{14} by $\sqrt{2}$. Thus $d_{15} \approx 2.2 \times 10^{-8}$ esu. Assuming an argon-ion laser pump at 0.5147μ we find $K = 2.7 \times 10^{-14}$ esu from the known index of refraction data for the degenerate wavelength $\lambda_0 = 1.029 \mu$. The lowest threshold occurs when signal and idler are nearly degenerate as can be seen from (2.41) when $\gamma = 0$. If we assume $l = 1$ cm in (2.42) and $\epsilon_1 = \epsilon_2 = 0.01$ then $P_3 = 11$ mW. This power must be in a single longitudinal as well as transverse mode to be effective. We shall discuss in the next section the reasonableness of this assumption of loss in the signal and idler modes.

3. EXPERIMENTS

3.1. Amplifier Experiment

A single-pass parameter-amplifier experiment was performed in the near field in order to check the gain expression (2.18) under conditions close to those needed for parametric oscillation. Near-field operation reduces the difficulty in superimposing the incident pump and signal beams and makes the comparison with (2.18) on an absolute basis more straightforward.

The experiment consisted of mixing an extraordinary wave-pump beam at $\lambda_3 = 0.5147 \mu$ from an argon-ion laser and an ordinary wave signal beam at $\lambda_1 = 1.1526 \mu$ from a He-Ne laser in a LiNbO_3 crystal to generate an ordinary wave idler at the difference frequency, where $\lambda_2 = 0.9299 \mu$. All wavelengths are quoted *in vacuum*. The experimental setup is shown in Fig. 1. The pump and signal beams were in the lowest order transverse modes. They were made collinear by a 45° dichroic mirror and then gently focused into a temperature-controlled¹⁵ LiNbO_3 crystal normal to the optic axis.

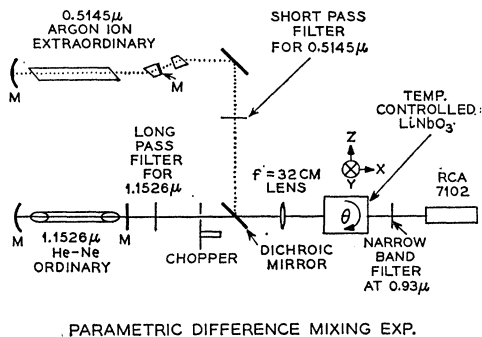


FIG. 1. Schematic of a parametric-difference-mixing experiment. The laser mirrors are indicated by M . The first prism in the argon laser selects the $0.5145\text{-}\mu$ line. The second prism following the argon laser makes the beam round.

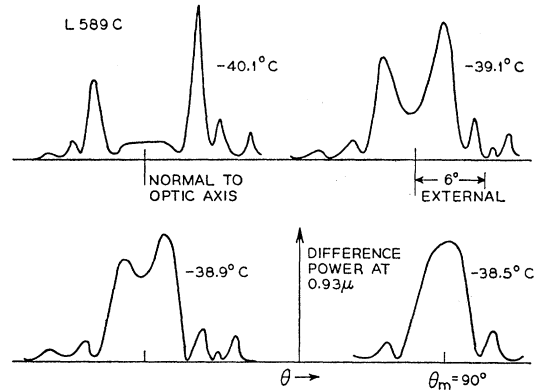


FIG. 2. Variation of the difference-frequency signal at 0.93μ with crystal rotation angle θ between the optical axis and the laser beams. At $T = -38.5^\circ\text{C}$ the phase-matching angle $\theta_m = 90^\circ$.

The crystal was placed in a Dewar to facilitate cooling. The crystal length $l = 0.835$ cm was small compared to the confocal parameters $b_3 = k_3 w_3^2 = 12$ cm and $b_1 = 14$ cm, thus assuring near-field operation.

By adjusting the crystal temperature to $T = -38.5^\circ\text{C}$ the dispersion and birefringence of the LiNbO_3 was varied to achieve phase matching normal to the optic axis. This is illustrated in Fig. 2 where the variation in phase-matching angle with crystal temperature is seen. At $T = -40.1^\circ\text{C}$ the pattern of idler power is essentially symmetrical about the normal to the optic axis ($\theta = 90^\circ$) and gives phase matching of the principal line at $\theta_m = 90 \pm 4^\circ$. At $T = -38.5^\circ\text{C}$ the principal phase-matching peaks coalesce at $\theta_m = 90^\circ$. Operation normal to the optic axis eliminates beam separation of ordinary and extraordinary beams due to double refraction. With $P_3 = 6.1$ mW and $P_1 = 3.8$ mW in the principal line at 1.15μ , we find experimentally that $P_2 = 1.2 \times 10^{-8}$ W when matched at $\theta_m = 90^\circ$. For our experiment $\gamma = 0.107$ and $K = 2.7 \times 10^{-14}$ esu as computed in Sec. 2.2. Substituting in (2.18) the theory predicts $P_2 = 0.8 \times 10^{-8}$ W. The agreement is satisfactory considering that our absolute power calibration at ω_2 was no better than a factor of 2 and the difficulties of beam alignment. In (2.17) and (2.18) we see that apart from the frequency factor the enhancement in signal power is equal to the generated idler power \bar{P}_2 and is thus quite small compared to the incident signal. For this reason no direct measurement of this enhancement was possible.

From the above numbers or (2.35) one obtains $\bar{P}_2/P_1 = 2.1 \times 10^{-6}$ as the parametric-amplifier gain whereas the parametric-oscillator gain for this pump power given by (2.34), yields $\Delta P_2/(P_1 P_2)^{1/2} = 0.003$. In this comparison we assumed

$$l^2/(w_1^2 + w_3^2) = l^2/(w_1^2 + w_2^2) = 2120.$$

Thus at low-gain levels the single-pass gain in the oscillator is sizably greater than in the amplifier for the same pump power.

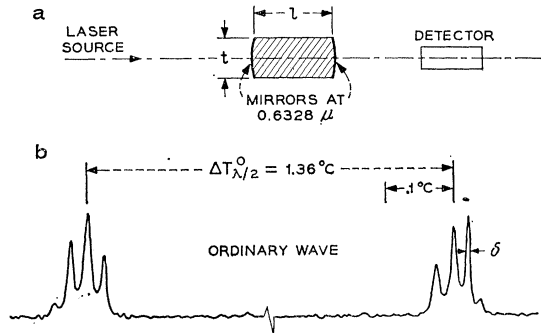


FIG. 3(a). Schematic of resonator used as a scanning interferometer. Detector measures resonator transmission from laser source at 0.6328μ . The resonator length is varied by temperature changes or by the application of a transverse electric field along the crystal optic axis which is normal to the resonator axis. (b). Transmission of crystal resonator at 0.6328μ versus temperature for ordinary ray in X crystal direction. Crystal length $l=0.55$ cm. Data indicate a one-way loss of $\epsilon=0.0174$ within the resonator. Because of frequency instabilities in the $0.6328\text{-}\mu$ laser and the low scan rate used in this experiment, the measured ϵ is probably too high (see Fig. 4).

It should be mentioned that in this experiment the pump power was in approximately a dozen longitudinal modes. This in no way affects the idler power as calculated from (2.18) since P_3 and P_1 are assumed to be uncorrelated and P_3 and P_1 are the total power of all the longitudinal modes at each frequency. The oscillator of course requires the pump to be in a single mode.

More recent difference-mixing experiments have shown that the phase-matching temperature of the above wavelengths varies for reasons not fully understood. In some crystals phase matching normal to the optic axis has occurred as high as $+80^\circ\text{C}$ and in others it has not been possible to observe phase matching even though the crystal has been cooled to -52°C which is the limit of our equipment. This is reflected in θ_m for SHG from the $1.1526\text{-}\mu$ laser which is found to vary from $\theta_m=65^\circ$ to 69° , respectively. The published index-of-refraction data³ indicate that $\theta_m=67.1^\circ$. (This was incorrectly given in Ref. 3.) If a high phase-matching temperature proves practical, the crystal will no longer have to be within a Dewar.

3.2. Q Measurements and Optical Path Length as a Function of Temperature and Electric Field

In order to demonstrate the possibility of resonators with low loss for signal and idler modes within bulk LiNbO_3 , several resonators were fabricated. The length l was approximately 1 cm and two curved surfaces were of 4-cm radius of curvature upon which multiple-layer dielectric reflectors were deposited, as illustrated in Fig. 3(a). The resonator was used as a scanning interferometer by varying either the temperature or electric field transverse to the resonator axis. In either case the optical path length nl must be changed by $\lambda/2$ to sweep through a complete resonance of the interferometer where λ is the free-space wavelength of

the exciting laser and n the index of refraction. As viewed by a detector measuring the resonator transmission, the ratio of spacing to peak width δ (in wavelength units) at half-power points is given by¹⁴

$$(\lambda/2)/\delta = \pi/\epsilon, \quad (3.1)$$

where ϵ is the equivalent one-way loss including one reflection within the resonator.

With the laser-exciting source at 0.6328μ and with 15 layers of ZnS-ThOF_2 the transmission spectrum versus temperature obtained is shown in Fig. 3(b). The fine structure is the resolution of longitudinal modes of the source laser. The data indicate a loss value of $\epsilon \approx 0.017$. Such low loss is not typical. Often bulk scattering loss can be observed visually with a $0.6328\text{-}\mu$ laser. This bulk scattering is possibly due to trapped gas bubbles which can sometimes be observed and other impurities. The elimination of bulk scattering losses requires careful preparation of the crystal.

As will be discussed in Sec. 4 with regard to simultaneous resonance of two frequencies, it is desirable to know the change in the optical path length $\Delta(nl)$ versus temperature and electric field. Such information is obtained from these scanning-interferometer-type experiments. Measurements were obtained for the change in temperature $\Delta T_{\lambda/2}^\circ$ and $\Delta T_{\lambda/2}^\circ$ for the ordinary and extraordinary wave to produce a change in optical path length

$$\Delta(nl) = n\Delta l + l\Delta n = \lambda/2. \quad (3.2)$$

The temperature change $\Delta T_{\lambda/2}^\circ\text{C}$ per half-wavelength will be inversely proportional to the crystal length l

$$\Delta T_{\lambda/2}^i = H^i/l, \quad i = o, e, \quad (3.3)$$

where $i=o, e$ represents the ordinary and extraordinary waves. The coefficient H^i in units of $^\circ\text{C cm}$ will be a function of wavelength λ and roughly proportional to λ but not strictly so since $\Delta(nl)/\Delta T$ is not independent of λ . The data summarized in Table I represent an average over several crystals and is probably accurate to 20%. The effect of Δl on $\Delta(nl)$ may be accounted for with thermal expansion data²¹ on LiNbO_3 to yield a measure of $\Delta n/\Delta T$. For the purposes of this paper it is $\Delta(nl)$ though that is of interest.

Consider now the scanning of the interferometer of Fig. 3(a) with electric field^{9,10} instead of temperature. The electro-optic effect in LiNbO_3 has been discussed

TABLE I. Temperature coefficient H and potential coefficient P to change the optical path length by $\lambda/2$ where $\lambda=0.6328 \mu$ for both an ordinary and extraordinary wave.

	H ($^\circ\text{C cm}$)	P (kV)
Ordinary	0.70	$P_{13}=5.0$ kV
Extraordinary	0.34	$P_{33}=1.77$ kV

²¹ K. Nassau, H. J. Levinstein, and G. M. Loiacono, J. Phys. Chem. Solids (to be published).

by Peterson *et al.*¹⁶ (though with multidomain material) and others.^{22,23} The change in optical path length between the reflectors is proportional to the dc electro-optic coefficient since we envision low scanning speeds (~ 60 cps). Referring to (3.2) one can write, following common practice,

$$\Delta(nl) \equiv l\Delta n = \lambda/2, \quad (3.4)$$

where the effect of Δl has been incorporated in the Δn as an effective change in index of refraction as a function of electric field. There are however low-frequency techniques which measure Δn in (3.2) directly and not $\Delta(nl)$. These exclude the contribution of Δl and thus give a dc electro-optic coefficient defined differently from the one based on (3.4) which is used here.

The axis of the resonator has been chosen normal to the crystal optic axis to avoid the limitations of double refraction as discussed earlier. To scan the signal-idler resonator with an electric field it is obviously most practical to apply an electric field transverse to the resonator axis. If the resonator axis is in the direction of the X crystal axis (a axis) one can show²² that the change in ordinary and extraordinary effective index of refractions are

$$\begin{aligned} \Delta(n^o) &= [- (n^o)^3/2] \{ r_{22}E_Y + r_{13}E_Z \}, \\ \Delta(n^e) &= [- (n^e)^3/2] r_{33}E_Z, \end{aligned} \quad (3.5)$$

where E_Y and E_Z are low frequency electric fields in the Y and Z crystal directions. Likewise if the resonator axis is in the direction of the Y crystal axis

$$\begin{aligned} \Delta(n^o) &= [- (n^o)^3/2] \{ -r_{22}E_Y + r_{13}E_Z \}, \\ \Delta(n^e) &= [- (n^e)^3/2] r_{33}E_Z. \end{aligned} \quad (3.6)$$

If one wishes to make use of the r_{22} coefficient it is clearly more desirable for practical reasons to choose the situation of (3.5) where the resonator axis is in the X direction and thus E_Y is a transverse electric field instead of along the resonator axis as in (3.6). A further motivation for having the resonator axis in the X direction is that we have found such an orientation to polish better than the Y direction.

Several workers^{16,22,23} have made measurements of the dc electro-optic and primary electro-optic coefficients of LiNbO_3 . Turner²³ has observed that the primary electro-optic (high-frequency) coefficient r_{13} is more than three times that of r_{22} . Furthermore E_Y will cause a very small rotation of the index ellipsoid. If the resonator is excited with an ordinary wave this causes some conversion to an extraordinary wave and thus a loss from the ordinary wave mode. Calculations show that this rotation loss is negligible compared with 0.1% per pass which is probably the best that we can achieve in the resonator due to bulk loss and mirror loss.

²² P. V. Lenzo, E. G. Spencer, and K. Nassau J. Opt. Soc. Am. 56, 633 (1966).

²³ E. H. Turner (unpublished).

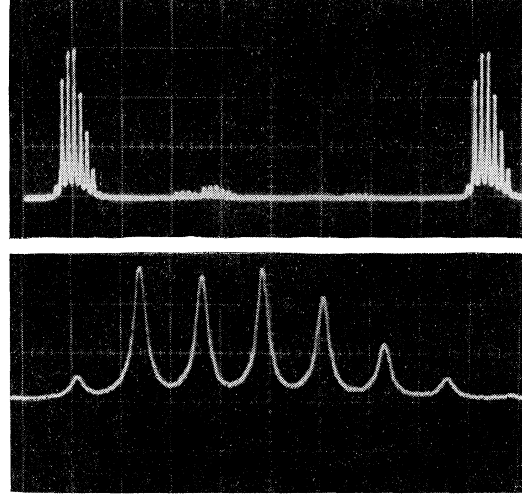


FIG. 4. Transmission of the extraordinary wave in the same crystal resonator used in Fig. 3(b) versus a transverse voltage along the optic axis. The indicated one-way loss is $\epsilon=0.011$. The sweep rate was 60 cps which was fast enough to avoid laser frequency instabilities. The horizontal calibration is 200 V/cm in the upper trace and 20 V/cm in the lower trace. The crystal thickness $l=0.45$ cm.

In the experiments described here only an electric field E_Z along the optic axis was employed. The transverse voltage, V in kilovolts required to change the optical path length by $\lambda/2$ will be proportional to the transverse crystal thickness t and inversely proportional to the resonator length l .

$$V = P(t/l). \quad (3.7)$$

The transverse electric field within the crystal will be

$$E_Z^i = (P^i/l) \text{ kV/cm}, \quad (3.8)$$

where $i=0, e$ represents ordinary and extraordinary waves. The proportionality constant P will have the dimensions of potential in units of kilovolts for convenience. The transverse electric field E_Z was swept at a 60-cps rate. Figure 4 shows the transmitted power at 0.6328μ versus voltage. The data clearly show the resolution of the longitudinal-mode structure of the exciting laser. The results are given in Table I for both an ordinary and an extraordinary polarization though of course for the signal and idler we are concerned only with ordinary waves. From the data of Fig. 4 and (3.1) we obtain that the loss per pass $\epsilon=0.011$. Not all crystals show this little loss.

The dc electro-optic coefficient is related to the potential coefficient P . From (3.4), (3.5), and (3.8) one obtains

$$\begin{aligned} - (n^o)^3 r_{13} P_{13}^o &= \lambda, \\ - (n^e)^3 r_{33} P_{33}^e &= \lambda. \end{aligned} \quad (3.9)$$

From Table I one obtains $|r_{13}| = 1.05 \times 10^{-9}$ cm/V and $|r_{33}| = 3.37 \times 10^{-9}$ cm/V. These numbers are approximately 20% above the results of Turner.²³ The difference is to be expected since Turner's measurements do

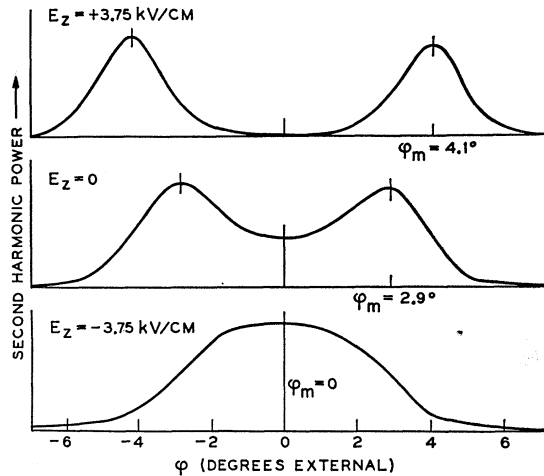


FIG. 5. Phase-matched SHG in LiNbO₃ from a 1.0798- μ laser versus angle $\varphi = (\pi/2) - \theta$ where θ is the angle between the optic axis and the fundamental beam direction in the XZ plane. The crystal temperature was precisely regulated at $T = 59^\circ\text{C}$ to obtain phase matching at near normal to the optic axis. Each curve represents a different value of electric field applied along the optic axis.

not include any effect of Δl in that they are at high frequency. The effect of Δl could be allowed for using the piezoelectric coefficients²⁴ but will not be in this paper. Furthermore, Turner²³ has observed that r_{13} and r_{33} have the same sign. In Sec. 3.3 we give a reason for assigning a + sign to r_{13} and r_{33} . It was observed qualitatively on one sample that P increased as the frequency decreased below 60 cps. This may account for a 20 \rightarrow 40% increase in measured P on several crystals. The data of Table I are the average of six crystal for which 60 cps seemed adequate. The frequency-dependent effect appears to be due to the RC time constant of the crystal.

3.3. Effect of Electric Field on Phase Matching

As is seen in Fig. 2 the phase-matching conditions for difference mixing can be effected by temperature variations.¹⁵ Likewise electric fields can similarly effect phase matching by a change in index of refraction of the ordinary and extraordinary waves [see (3.5) and (3.6)]. This is important in connection with simultaneous resonance to be discussed in Sec. 4. As a simple direct measure of the effect we have observed the change in phase-matching angle with electric field in second-harmonic generation of the 1.0798- μ He-Ne laser as seen in Fig. 5. To provide adequate sensitivity the LiNbO₃ crystal temperature was adjusted so that phase matching occurred normal to the optic axis. In these experiments only an E_z component of electric field was used.

In BADK¹² Eq. (2.9), the phase-matching angle θ_m is measured from the optic axis. In terms of the angle

$\varphi_m = (\pi/2) - \theta_m$ as measured from the normal to the optic axis one can write

$$\sin^2 \varphi_m = \left(\frac{n_2^o}{n_1^o} \right)^2 \frac{n_1^o + n_2^o}{n_2^o + n_2^e} \left(1 - \frac{D^o}{B} \right), \quad (3.10)$$

where

$$\begin{aligned} D^o &= n_2^o - n_1^o, \\ B &= n_2^o - n_2^e. \end{aligned} \quad (3.11)$$

In the limit of $\varphi_m \ll 1$

$$d(\varphi_m^2)/dE \approx -d(D^o/B)/dE. \quad (3.12)$$

From the data of Fig. 5 note that $\Delta(\varphi_m^2)$ is linear with E_z . One obtains

$$d(D^o/B)/dE = -1.36 \times 10^{-7} \text{ cm/V}. \quad (3.13)$$

The electric field in this experiment was applied both as a steady dc voltage and as a square wave at 390 cps in phase with the chopped fundamental beam. The results were indistinguishable on the one crystal tested and thus low-frequency effects were absent.

The quantity $d(D^o/B)/dE$ may also be computed from the electro-optic coefficients if we neglect the effect of Δl in the previous measurements and thus assume r_{13}, r_{33} to represent a change Δn in the index of refraction only. The effect of Δl could be allowed for using the piezoelectric coefficients²⁴ but this will not be included here. At $\varphi_m \sim 0$

$$\frac{d}{dE} \left(\frac{D^o}{B} \right) \approx \frac{1}{D^o} \frac{d(D^o - B)}{dE} = \frac{1}{D^o} \frac{d(n_2^e - n_1^o)}{dE}. \quad (3.14)$$

From (3.5) allowing only for an E_z component one obtains

$$\frac{d}{dE} \left(\frac{D^o}{B} \right) = - \frac{(n_1^o)^3 (r_{33} - r_{13})}{2D^o} = -1.52 \times 10^{-7} \text{ cm/V}, \quad (3.15)$$

where we have taken r_{13} and r_{33} as positive and neglected any changes with wavelength. The values $n_1^o = 2.233$ and $D^o = 0.085$ were used. The agreement between (3.15) and (3.13) corroborates the assignment of + signs to r_{13} and r_{33} . By convention a positive electric field points from the + to the - potential. In the experiment of Fig. 5 the +c axis was determined pyroelectrically and is the direction of the ferroelectric polarization vector. The electric field was defined as positive when pointing in the direction of the +c axis.

4. SIMULTANEOUS RESONANCE

In a parametric oscillator simultaneous resonance of signal and idler is necessary for achieving the lowest threshold for a given pump power. We envision the pump making a single pass in one direction through the signal and idler resonator. The curved mirror surfaces are assumed to be ground on the crystal with the resonator axis taken normal to the crystalline optic

²⁴ A. W. Warner, in Proceedings of the Nineteenth Frequency Control Symposium, 1965, USAERL, Ft. Monmouth, New Jersey.

axis. This precludes the use of crystal rotation as a means of phase matching, although under different circumstances this may be a useful technique. The dielectric reflectors deposited on the curved surfaces will be highly reflecting at the signal and idler frequencies which in practice will probably be no more than 30% from degenerate. These mirrors will be reasonably (greater than say 80%) transparent at the pump wavelength.

In what follows we shall assume the pump wavelength to be the 0.5147- μ line of the argon-ion laser. The sum of the signal and idler frequencies is equal to the pump frequency. What we call signal and idler is arbitrary, but in this paper the signal has been thought of as the lower frequency which was the case in the difference-mixing experiment.

4.1. Statement of the Problem

Simultaneous resonance of signal and idler requires that the number of half-wavelengths of frequencies ω_1 and ω_2 both be integral. Define the quantities

$$\begin{aligned} m_1 &= 2n_1 l_1 / \lambda_1 = \omega_1 n_1 l_1 / \pi c, \\ m_2 &= 2n_2 l_2 / \lambda_2 = \omega_2 n_2 l_2 / \pi c, \end{aligned} \quad (4.1)$$

where m_1, m_2 are considered to be continuous variables taking on integral values when resonance is achieved. Note that the resonator is considered to have a different length l at each frequency. We shall only consider in this paper differences between l_1, l_2 of the order of a wavelength or so since we assume signal and idler to share the same mirror surfaces. The difference in resonator length will be the result of the shift in the effective mirror plane of the dielectric reflectors with frequency. Let

$$\begin{aligned} l_1 &= l_0 [1 + f_1(\lambda) / l_0], \\ l_2 &= l_0 [1 + f_2(\lambda) / l_0], \end{aligned} \quad (4.2)$$

where $f_1(\lambda)$ and $f_2(\lambda)$ are of order of one wavelength.

The requirements on index of refraction for phase matching are given by (2.29) and (2.28). Assume as a first-order approximation in (2.28) that the change in index of refraction n_1, n_2 about n_0 is linear with frequency. Expand the index of refraction about n_0 and define

$$D = \omega_0 (dn^\circ / d\omega) |_{\omega_0}. \quad (4.3)$$

This is a generalization of the dispersion in index of refraction used in SHG as given in (3.11) as can be seen from (4.3) since if $\Delta\omega = \omega_0$ then

$$D = \Delta n^\circ = n^\circ(2\omega_0) - n^\circ(\omega_0) = D^\circ. \quad (4.4)$$

From (2.28) and (4.3) one can show that

$$\begin{aligned} n_2^\circ &= n_0^\circ + \gamma D, \\ n_1^\circ &= n_0^\circ + \gamma D, \end{aligned} \quad (4.5)$$

where

$$\zeta n_0^\circ = \gamma D. \quad (4.6)$$

The phase-matching condition (2.29) for the parametric oscillator can then be written with (4.6) as

$$\gamma^2 = (n_3^\circ - n_0^\circ) / D = (D^\circ - B) / D, \quad (4.7)$$

where

$$D^\circ - B = (n_3^\circ - n_0^\circ) - (n_3^\circ - n_3^\circ). \quad (4.8)$$

B is the birefringence normal to the optic axis at the pump frequency and D° represents the dispersion of the ordinary wave between ω_3 and ω_0 . If $B > D^\circ$ then γ is imaginary indicating that phase-matching normal to the optic axis is not possible at that temperature and electric field for the pump frequency chosen.

If the index of refraction is linear with frequency over the frequency range ω_0 to $\omega_3 = 2\omega_0$ then

$$D^\circ = D. \quad (4.9)$$

This is only a fair approximation in that from (4.3) and the data of Ref. 3, one obtains $D = 0.071$ and $D^\circ = n_3^\circ - n_0^\circ = 0.097$, when $\lambda_0 = 1.029 \mu$. Also $B = n_3^\circ - n_3^\circ = 0.094$. In this paper the approximation of (4.9) will be made in subsequent calculations.

With (2.3) and (4.5) one can write (4.1) as

$$\begin{aligned} m_1 &= (1 - \gamma) [1 - \gamma D / n_0^\circ] [1 + f_1(\lambda) / l_0] m_0, \\ m_2 &= (1 + \gamma) [1 + \gamma D / n_0^\circ] [1 + f_2(\lambda) / l_0] m_0, \end{aligned} \quad (4.10)$$

where

$$m_0 = 2n_0^\circ l_0 / \lambda_0 = \omega_0 n_0^\circ l_0 / \pi c \quad (4.11)$$

is the number of half wavelengths at the degenerate frequency. m_0 is only a convenient mathematical variable and need not be an integer. Typically $m_0 \approx 45\,000$ if $l = 1$ cm.

For simultaneous resonance we require that m_1 and m_2 both be integral. As will be seen it is more convenient to deal with $m_2 + m_1$ and $m_2 - m_1$ and thus one may write

$$\begin{aligned} m_2 - m_1 &= m_0 \left\{ 2\gamma \left(1 + \frac{D}{n_0^\circ} \right) + \frac{f_2 - f_1}{l} \left(1 + \frac{\gamma^2 D}{n_0^\circ} \right) \right. \\ &\quad \left. + \frac{f_2 + f_1}{l} \gamma \left(1 + \frac{D}{n_0^\circ} \right) \right\}, \\ m_2 + m_1 &= m_0 \left\{ 2 \left(1 + \frac{\gamma^2 D}{n_0^\circ} \right) + \frac{f_2 + f_1}{l} \left(1 + \frac{\gamma^2 D}{n_0^\circ} \right) \right. \\ &\quad \left. + \frac{f_2 - f_1}{l} \gamma \left(1 + \frac{D}{n_0^\circ} \right) \right\}. \end{aligned} \quad (4.12)$$

In the simplest approximation of (4.12) one obtains

$$\begin{aligned} m_2 - m_1 &= 2\gamma m_0, \\ m_2 + m_1 &= 2m_0, \end{aligned} \quad (4.13)$$

since $D/n_0^\circ \approx 0.03 \ll 1$.

A variety of means can be used to adjust the values of m_1 and m_2 to give simultaneous resonance. As

mentioned in Sec. 3, the temperature and electric field can be used to vary the optical path length and hence m_0 . Also, the application of stress would vary the optical path length though this will not be considered in this paper. Likewise a change in the pump frequency $\omega_s=2\omega_0$ changes m_0 . All of these parameters likewise affect the phase-matching condition and thus the signal and idler frequencies as seen in (4.7) and (2.3) through their influence on the indices of refraction.

In a parametric amplifier the adjustment of a single variable (usually temperature) provides continuous variation of the signal and idler frequencies that are phase matched while remaining normal to the optic axis. In a parametric oscillator the need for simultaneous resonance and phase matching requires in general two variables. As will be seen there are then a large number of such coincidences over the frequency spectrum in varying density depending on γ . If three variables are adjusted it can be shown that any desired frequency (in a limited range) can be phase matched and made simultaneously resonant thus providing for continuous tuning of a parametric oscillator.

Consider now how much the quantities m_1 and m_2 must be adjusted to achieve simultaneous resonance. It will be seen that the difference m_2-m_1 and the sum m_2+m_1 can be adjusted well within practical limits to achieve simultaneous resonance. If the difference m_2-m_1 and the sum m_2+m_1 are integers, this is not quite enough to assure that m_2 and m_1 are both integers. The one exception occurs when both m_1 and m_2 are integers plus $\frac{1}{2}$ since then both m_2-m_1 and m_2+m_1 are still integral. This difficulty can be overcome by extending the range of variation of m_2-m_1 and m_2+m_1 . Consequently the maximum adjustment required to achieve integral values are

$$\begin{aligned}\Delta(m_2-m_1) &\leq 1, \\ \Delta(m_2+m_1) &\leq 2,\end{aligned}\quad (4.14)$$

or the reverse where

$$\begin{aligned}\Delta(m_2+m_1) &\leq 1, \\ \Delta(m_2-m_1) &\leq 2.\end{aligned}\quad (4.15)$$

Either set of maximum adjustments is satisfactory but for simplicity we consider only (4.14).

From (4.13) one can express the changes in m_2-m_1 and m_2+m_1 in terms of the variables E , T , and ω_0 as

$$\begin{aligned}\frac{1}{2}d(m_2-m_1) &= \left[m_0 \frac{\partial \gamma}{\partial E} + \gamma \frac{\partial m_0}{\partial E} \right] dE + \left[m_0 \frac{\partial \gamma}{\partial T} + \gamma \frac{\partial m_0}{\partial T} \right] dT \\ &\quad + \left[m_0 \frac{\partial \gamma}{\partial \omega_0} + \gamma \frac{\partial m_0}{\partial \omega_0} \right] d\omega_0,\end{aligned}\quad (4.16)$$

and

$$\begin{aligned}\frac{1}{2}d(m_2+m_1) &= (\partial m_0/\partial E)dE + (\partial m_0/\partial T)dT \\ &\quad + (\partial m_0/\partial \omega_0)d\omega_0.\end{aligned}\quad (4.17)$$

To evaluate (4.16) and (4.17) requires the knowledge of the rates of change of γ and m_0 with E , T , and ω_0 . These will be found in Secs. 4.2, 4.3, and 4.4. Finally in 4.5 the specific adjustments for simultaneous resonance will be discussed.

4.2. Effect of Temperature on Phase Matching

The change in the phase-matched frequencies ω_1 and ω_2 with temperature at conditions of constant E and ω_0 is obtained from (4.7) in the approximation of (4.9) as

$$\frac{\partial \gamma^2}{\partial T} = -\frac{\partial}{\partial T} \left(\frac{B}{D} \right) \approx \frac{1}{D} \frac{\partial(D-B)}{\partial T} = +C^2, \quad (4.18)$$

where for $\gamma^2 \ll 1$, $B \approx D$. C^2 is taken as a constant to be evaluated. From Ref. 15,

$$\partial(D-B)/\partial T = +5.7 \times 10^{-5}/^\circ\text{C}, \quad (4.19)$$

and from Ref. 3, $D=0.071$ from which $C^2=8.0 \times 10^{-4}$ and $C=0.028$ per $(^\circ\text{C})^{1/2}$. The solution of the differential equation (4.18) is

$$\gamma = +C(T-T_0)^{1/2}. \quad (4.20)$$

The shift in the idler or signal frequencies from the degenerate frequency $1/\lambda_0=9718 \text{ cm}^{-1}$ is

$$\Delta(1/\lambda) = \pm 274(T-T_0)^{1/2} \text{ cm}^{-1}. \quad (4.21)$$

As a typical example note that for $\gamma=0.1$, $T-T_0=12.5^\circ\text{C}$. If $T < T_0$, phase matching normal to the optic axis is not possible as there is too much birefringence. Phase matching is only possible at $\theta_m < 90^\circ$ which would reduce the birefringence but bring in double refraction.

In (4.11) m_0 is the number of half wavelengths at the degenerate frequency for the ordinary ray along the resonator axis. From (3.3) and (4.11) one may write

$$\partial m_0/\partial T = l/H^\circ. \quad (4.22)$$

From (4.18) and (4.22) one observes for the numerical values given in this paper that

$$m_0(\partial \gamma/\partial T) \gg \gamma(\partial m_0/\partial T). \quad (4.23)$$

4.3. Effect of Electric Field on Phase Matching

The change in γ and thus ω_1 and ω_2 with electric field at conditions of constant E and ω_0 is obtained from (4.7) and (4.9) as

$$\begin{aligned}\partial \gamma^2/\partial E &= -\partial(D/B)/\partial E \\ &= +(B/D)^2 \partial(D/B)/\partial E.\end{aligned}\quad (4.24)$$

Previously in Sec. 3.3 we measured $d(D^\circ/B)/dE$ at the nearby wavelength of 1.08μ instead of where desired at 1.029μ . Assuming $D=D^\circ$ as in (4.9), neglecting differences due to wavelength and setting $B=D$ for $\gamma^2 \ll 1$

one obtains

$$\partial\gamma^2/\partial E = +R^2 = +1.36 \times 10^{-7} \text{ cm/V}. \quad (4.25)$$

From (3.8) and (4.11) one may write

$$\partial m_0/\partial E = l/P^0, \quad (4.26)$$

and as before with temperature one may show numerically that

$$m_0(\partial\gamma/\partial E) \gg \gamma(\partial m_0/\partial E). \quad (4.27)$$

4.4. Effect of Pump-Frequency Variations on Phase Match

One further possibility for adjustment of the phase-matching condition is to tune the pump frequency over a fraction of the Doppler linewidth. Expand the known³ index-of-refraction data in terms of a polynomial in frequency squared for both ordinary and extraordinary waves as

$$\begin{aligned} n^o &= p^o + q^o\nu^2 + r^o\nu^4, \\ n^e &= p^e + q^e\nu^2 + r^e\nu^4, \end{aligned} \quad (4.28)$$

where the angular frequency

$$\omega = 2\pi c\nu, \quad (4.29)$$

and $\nu = 1/\lambda$ in units of reciprocal microns. One can obtain a functional form for γ^2 in (4.7) as a function of the degenerate wavelength λ_0 . Calculations indicate that

$$\partial\gamma^2/\partial(\nu^2) \approx (p^o - p^e)/3q^o\nu^4 = +0.76/\nu^4, \quad (4.30)$$

where now $\nu = 1/\lambda_0$. We do not give in this paper the value of the coefficients in (4.28) and the representation for $\gamma^2(\nu)$ since existing index-of-refraction data³ are not precisely applicable to all crystals as is apparent from the variation of the phase-matching temperature mentioned in Sec. 3.1. The rate of change of γ^2 with ν^2 would appear to be insensitive to the variations observed.

From (4.11) one can show that

$$\partial m_0/\partial\nu \approx m_0/\nu \quad (4.31)$$

and for $\gamma < 0.25$ that

$$m_0(\partial\gamma/\partial\nu) \gg \gamma(\partial m_0/\partial\nu). \quad (4.32)$$

These relations will be needed in the next section.

4.5. Adjustments for Simultaneous Resonance

This section demonstrates the existence of numerous simultaneous resonances with a series of adjustments that are mathematically rather than experimentally convenient. In practice the experiment will probably be performed differently. The procedure consists of first adjusting $m_2 - m_1$ to an integral value and then varying $m_2 + m_1$ until it becomes integral without having changed $m_2 - m_1$. As described above this results in integral values of m_1 and m_2 separately and

therefore simultaneous resonance of signal and idler under phase-matched conditions.

Consider adjusting $m_2 - m_1$ to an integral value starting from some initial condition of E , T , and ω_0 . According to (4.14) this can be accomplished by changing $m_2 - m_1$ by at most unity. That is,

$$\Delta(m_2 - m_1) = 1, \quad (4.33)$$

corresponding to a change in the difference of the number of half-wavelengths at the idler and signal frequencies of unity. The change in γ , $\Delta\gamma$, required to satisfy (4.33) can be obtained from (4.16) using the approximations (4.23), (4.27), and (4.32) as

$$\Delta\gamma = 1/2m_0 \quad (4.34)$$

which is one-half the fractional frequency change between modes of the resonator. Assuming $l = 1$ cm, $\Delta\gamma = 1.1 \times 10^{-5}$.

Such a change $\Delta\gamma$ can be achieved with a small change in temperature, electric field, or pump frequency. Considering temperature, at $T = T_0$ where $\gamma = 0$ one obtains from (4.18) and (4.34) that $\Delta T = 1.5 \times 10^{-7} \text{ }^\circ\text{C}$ and at $\gamma = 0.1$, $\Delta T = 0.28 \times 10^{-2} \text{ }^\circ\text{C}$. Similarly from (4.25) one obtains a change in electric field $\Delta E = 0.001$ V/cm at $\gamma = 0$ and 61 V/cm at $\gamma = 0.1$ as being required to produce $\Delta\gamma$ as given by (4.34). Likewise from (4.30) one can show that a change in degenerate frequency of 26 kc/sec is required at $\gamma = 0$ to satisfy (4.34) and at $\gamma = 0.1$ a change in degenerate frequency of 0.47 kMc/sec is required. This latter number is within a practical range of tunability of the argon laser since the Doppler linewidth is approximately 4 kMc/sec and thus tuning the pump frequency by 1 kMc/sec does not seem unreasonable.

These changes in $\Delta\gamma$ using temperature, electric field, or frequency if applied separately, as above, can make $m_2 - m_1$ integral, but result in finite changes in signal and idler frequencies. If, however, a parametric oscillator is desired at some particular frequency ω_2 one can, for example, change T by dT and ω_0 by $d\omega_0$ in the proper ratio (with $dE = 0$) such that $m_2 - m_1$ becomes integral while maintaining ω_2 a constant. That is

$$d\omega_2 = d[(1 + \gamma)\omega_0] = 0. \quad (4.35)$$

Since $m_2 - m_1$ is assumed to be integral and held constant one has from (4.13)

$$\frac{1}{2}d(m_2 - m_1) = d(\gamma m_0) = 0. \quad (4.36)$$

One can then adjust $m_2 + m_1$ using the three variables E , T , and ω_0 such that $m_2 + m_1$ becomes an integer while ω_2 and $m_2 - m_1$ remain constant. From (4.13) and (4.14) the maximum adjustment required to make $m_2 + m_1$ integral can be written

$$\frac{1}{2}d(m_2 + m_1) = dm_0 \leq 1. \quad (4.37)$$

Sweeping m_2+m_1 over this range while holding m_2-m_1 integral will assure that at some point m_1 and m_2 will each be integral. Equations (4.35), (4.36), and (4.37) represent three equations and three variables (unknowns) and thus have a solution.

We shall not in this paper discuss the general solution of these equations as our intention is only to demonstrate that there are conditions of simultaneous resonance. Consequently, we consider in detail the simpler situation involving only two of the possible variables (say E and T with ω_0 constant) governed by (4.36) and (4.37). We relax on condition (4.35) and tolerate small changes in signal and idler frequency. We might equally as well consider the variables E and ω_0 with T held constant. Assuming though that $d\omega_0=0$, from (4.36) and (4.16) one obtains

$$dT/dE = -[\partial(\gamma m_0)/\partial E]/[\partial(\gamma m_0)/\partial T], \quad (4.38)$$

which represents the ratio of the changes in T and E to keep m_2-m_1 an integer while adjusting m_2+m_1 . From (4.17), (4.37), and (4.38),

$$dm_0 = \frac{m_0[(\partial m_0/\partial E)(\partial \gamma/\partial T) - (\partial m_0/\partial T)(\partial \gamma/\partial E)]}{m_0(\partial \gamma/\partial T) + \gamma(\partial m_0/\partial T)} \times dE \leq 1. \quad (4.39)$$

This result specifies the change in electric field required to change m_2+m_1 by 2 while keeping m_2-m_1 an integer. With (4.23) rewrite (4.39) as

$$\Delta E \left(\frac{\partial m_0}{\partial E} - \frac{\partial m_0}{\partial T} \frac{\partial \gamma/\partial E}{\partial \gamma/\partial T} \right) \leq 1. \quad (4.40)$$

Using (4.18), (4.22), (4.24), and (4.26) one obtains

$$(l/P^0)\Delta E_z[1-PR^2/HC^2] \leq 1. \quad (4.41)$$

From the values given in this paper $PR^2/HC^2=1.21$ and thus if $l=1$ cm, $\Delta E_z \leq 23.8$ kV/cm. Actually no more than half this electric field would be required if one adjusts m_2+m_1 in the direction of the nearest integral value of m_2+m_1 for which m_1 and m_2 are each integral. The variation of E_z described by (4.41) assumes that the temperature T is simultaneously adjusted according to (4.38) to maintain m_2-m_1 integral. It is straightforward to show that a 23.8 kV/cm change in electric field would require a temperature change of 4.05°C to satisfy (4.36).

In any experimental situation it is most unlikely that adjustments will be made in the fashion described

above. For example one might sweep the electric field at 60 cps and adjust the temperature and/or the pump frequency at some slow rate until oscillation was achieved. If one allows m_2-m_1 to change over many integral values and thus ω_1 and ω_2 to vary significantly, one will achieve simultaneous resonance with smaller changes in the electric field.

The above discussion assumes perfect phase matching and infinite Q of the signal-idler resonator. Assuming simultaneous resonance and only two variables, say E and T or E and ω_0 , the smallest discrete change in the signal and idler frequency was given by (4.33). In practice, smaller changes in frequency will probably be possible with $\Delta(m_2-m_1)=0$ and small variations in temperature and electric field by allowing small deviations from phase matching and recognizing that finite resonator Q will relax the requirement that m_2 and m_1 be exactly integral. Furthermore, as previously mentioned if we allow three variables then continuous tuning of a parametric oscillator will be possible.

5. CONCLUSIONS

Parametric amplification has been observed and found to be in agreement with theory. Calculations of oscillator thresholds indicate that cw operation should be possible with gas-laser pump sources. Simultaneous resonance should be achievable with signal and idler sharing the same reflectors. Furthermore, it is shown that the geometry permits continuous tunability if three adjustments are used.

The parametric-oscillator-threshold theory presented here does not include the effects of diffraction which will probably raise the threshold somewhat. This can be included by using other techniques.¹³

ACKNOWLEDGMENTS

Without the cooperation of K. Nassau and co-workers in growing bigger and better crystals, this work would not be possible. We are especially grateful to J. P. Gordon for numerous helpful discussions. We have benefited from discussions with D. A. Kleinman and G. E. Peterson. Critical reading of the manuscript by A. N. Chester, J. A. Giordmaine, R. C. Miller, and R. G. Smith was very helpful. The able technical assistance of A. E. DiGiovanni, J. M. Dziedzic, and H. L. Carter with the experiments is appreciated. We thank D. L. Perry and L. B. Hooker for all the dielectric mirrors.

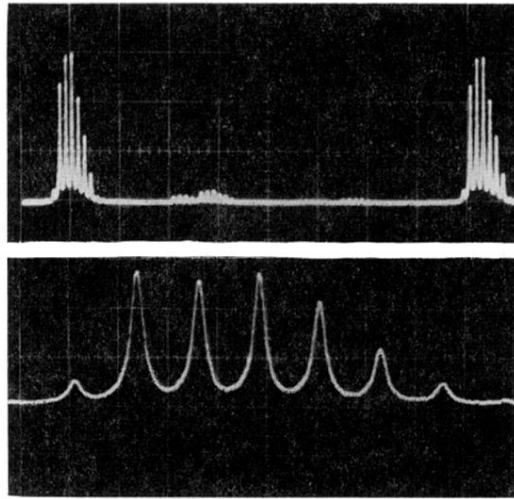


FIG. 4. Transmission of the extraordinary wave in the same crystal resonator used in Fig. 3(b) versus a transverse voltage along the optic axis. The indicated one-way loss is $\epsilon=0.011$. The sweep rate was 60 cps which was fast enough to avoid laser frequency instabilities. The horizontal calibration is 200 V/cm in the upper trace and 20 V/cm in the lower trace. The crystal thickness $l=0.45$ cm.